Analysis of Slotlines and Microstrip Lines on Anisotropic Substrates

Masahiro Geshiro, *Member, IEEE*, Seikou Yagi, and Shinnosuke Sawa, *Member, IEEE*

Abstract—**The propagation characteristics of the dominant mode in slotlines, as well as in microstrip lines, on anisotropic substrates are studied. The dielectric tensor in the substrate may have nondiagonal elements which represent misalignment, on the substrate surface, between the material coordinate system and the waveguide coordinate system. The analysis is devoted to the slotline and is based on Galerkin's method applied in the spectral domain. Numerical results are presented for a sapphire substrate and a boron nitride substrate. It is found that the coordinate misalignment on the substrate surface has a significant influence on the propagation characteristics of the slotline.**

I. Introduction

Dielectric anisotropy is observed in various substrate materials for microwave and millimeter-wave integrated circuits. The anisotropy in such crystalline materials as sapphire and boron nitride is a natural property. On the other hand it is adventitiously introduced in polytetrafluoroethylene-based substrates. Whether the anisotropy is natural or not, the significance of rigorous analyses of planar waveguide structures on anisotropic substrates increases as the operating frequency gets higher. Existing dynamic methods employed to obtain the propagation characteristics for various waveguide structures are summarized in [1]. In addition, the dispersive properties of finlines have been investigated by means of a spectral-domain method, and a perturbation-iteration solution based on potential theory has been developed for analyzing microstrip dispersion [2], [3]. However, the anisotropy chosen in the above investigations is characterized by a diagonal tensor permittivity.

Concerning dynamic analyses taking nondiagonal elements of the tensor into accounts, a few studies have been reported to date [4], [5]. The published papers, however, relate exclusively to microstrip lines, presenting no detailed numerical results for the propagation characteristics. This paper presents an analysis of slotlines, as well as microstrip lines, on anisotropic dielectric substrates, with numerical results for various values of structural and material parameters. The tensor permittivity in the substrate may have nondiagonal elements which represent misalignment, on the substrate surface, between the material coordinate system and the waveguide coordinate system. The analytical procedure is based on Galerkin's method applied in the spectral domain [6].

Manuscript received May 1, 1990; revised August 14, 1990.
M. Geshiro and S. Sawa are with the Department of Electronics Engineering, Ehime University, Bunkyo-3, Matsuyama, Ehime 790, Japan.
S. Yagi was with the Department of Electronics Engineering, Ehime University, Ehime, Japan. He is now with the NTT Data Communications Systems Corporation, 66-2, Horikawa, Saiwai-ku, Kawasaki, Kanagawa 210, Japan.
IEEE Log Number 9040557.

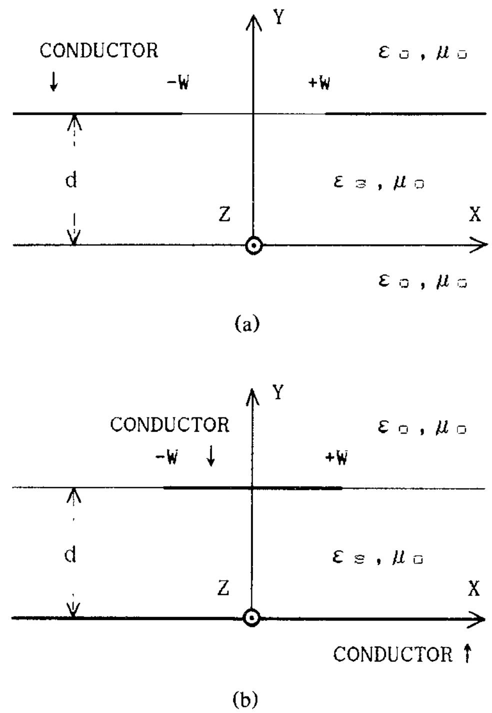

Fig. 1. Cross-sectional view of the waveguide structures: (a) slotline and (b) microstrip line.

II. Waveguide Structure and Formulation

The waveguide structures under consideration are shown in Fig. 1 together with the coordinate system for the analysis. The direction of propagation coincides with the z axis. In the substrate region (region I: $0 < y < d$), the dielectric tensor is assumed to be

$$\epsilon_s = \epsilon_0 \begin{pmatrix} \epsilon_{xx} & 0 & \epsilon_{xz} \\ 0 & \epsilon_{yy} & 0 \\ \epsilon_{zx} & 0 & \epsilon_{zz} \end{pmatrix} \tag{1}$$

$$\begin{cases} \epsilon_0\epsilon_{xx} = \epsilon_{\xi\xi}\cos^2\theta + \epsilon_{\zeta\zeta}\sin^2\theta \\ \epsilon_0\epsilon_{yy} = \epsilon_{\eta\eta} \\ \epsilon_0\epsilon_{zz} = \epsilon_{\xi\xi}\sin^2\theta + \epsilon_{\zeta\zeta}\cos^2\theta \\ \epsilon_0\epsilon_{xz} = \epsilon_0\epsilon_{zx} = (\epsilon_{\zeta\zeta} - \epsilon_{\xi\xi})\sin\theta\cos\theta \end{cases} \tag{2}$$

where ϵ_0 is the free-space permittivity, $(\epsilon_{\xi\xi}, \epsilon_{\eta\eta}, \epsilon_{\zeta\zeta})$ are principal dielectric constants in the material coordinate system (ξ, η, ζ), and θ is the angle between the z axis and the ζ axis.

0018-9480/91/0100-0064$01.00

The wave equations for the longitudinal field components in region I are derived from Maxwell's equations as

$$\left\{\frac{j\alpha\beta}{\omega\mu_0}\left(\kappa_x^2-\kappa_y^2\right)-j\kappa_y^2\omega\epsilon_0\epsilon_{xz}\right\}\frac{d\tilde{E}_{z1}}{dy}+\left\{\kappa_y^2\frac{d^2}{dy^2}-\kappa_x^2\left(\alpha^2-\kappa_y^2\right)\right\}\tilde{H}_{z1}=0 \quad (3)$$

$$\left\{\kappa_x^2\epsilon_{yy}\frac{d^2}{dy^2}-\kappa_y^2\left(k_0^2\epsilon_{xz}^2+2\alpha\beta\epsilon_{xz}-\kappa_x^2\epsilon_{zz}+\alpha^2\epsilon_{xx}\right)\right\}\tilde{E}_{z1}+\left\{\frac{j\alpha\beta}{\omega\epsilon_0}\left(\kappa_x^2-\kappa_y^2\right)-j\kappa_y^2\omega\mu_0\epsilon_{xz}\right\}\frac{d\tilde{H}_{z1}}{dy}=0 \quad (4)$$

where

$$\kappa_x^2=k_0^2\epsilon_{xx}-\beta^2 \quad (5)$$

$$\kappa_y^2=k_0^2\epsilon_{yy}-\beta^2 \quad (6)$$

$$k_0^2=\omega^2\epsilon_0\mu_0. \quad (7)$$

In the above equations, ω is the operating frequency and μ_0 the free-space permeability. $\tilde{E}_{z1}$ and $\tilde{H}_{z1}$ are the Fourier transforms of E_{z1} and H_{z1}. For example,

$$\tilde{E}_{z1}(\alpha,y)=\int_{-\infty}^{+\infty}E_{z1}(x,y)\exp(j\alpha x)\,dx. \quad (8)$$

The propagation factor $\exp[j(\omega t-\beta z)]$ has been omitted.

The following formulation is devoted to the slotlines. The solution for (3) and (4) is expressed in terms of four elementary waves as

$$\begin{cases}\tilde{E}_{z1}=A_1\exp(\gamma_1 y)+B_1\exp(-\gamma_1 y)\\ \qquad -jZ\{C_1\exp(\gamma_2 y)+D_1\exp(-\gamma_2 y)\}\\ \tilde{H}_{z1}=-jY\{A_1\exp(\gamma_1 y)-B_1\exp(-\gamma_1 y)\}\\ \qquad +C_1\exp(\gamma_2 y)-D_1\exp(-\gamma_2 y)\end{cases} \quad (9)$$

where A_1, B_1, C_1, and D_1 are unknown amplitude coefficients and

$$Y=\frac{\gamma_1\left\{\alpha\beta\left(\kappa_x^2-\kappa_y^2\right)-\kappa_y^2k_0^2\epsilon_{xz}\right\}}{\omega\mu_0\left\{\kappa_y^2\gamma_1^2-\kappa_x^2\left(\alpha^2-\kappa_y^2\right)\right\}} \quad (10)$$

$$Z=\frac{\gamma_2\left\{\alpha\beta\left(\kappa_x^2-\kappa_y^2\right)-\kappa_y^2k_0^2\epsilon_{xz}\right\}}{\omega\epsilon_0\left\{\kappa_x^2\epsilon_{yy}\gamma_2^2-\kappa_y^2\left(k_0^2\epsilon_{xz}^2+2\alpha\beta\epsilon_{xz}-\kappa_x^2\epsilon_{zz}+\alpha^2\epsilon_{xx}\right)\right\}}. \quad (11)$$

The squares of the transverse wavenumbers, γ_1^2 and γ_2^2, are the solutions for the following quadratic equation with respect to γ^2:

$$\begin{aligned}&\kappa_x^2\kappa_y^2\epsilon_{yy}\gamma^4+\Big[\kappa_x^4\left(\kappa_y^2-\alpha^2\right)\epsilon_{yy}\\ &\quad-\kappa_y^4\left(k_0^2\epsilon_{xz}^2+2\alpha\beta\epsilon_{xz}-\kappa_x^2\epsilon_{zz}+\alpha^2\epsilon_{xx}\right)\\ &\quad+\left\{\alpha\beta\left(\kappa_x^2-\kappa_y^2\right)/k_0-\kappa_y^2k_0\epsilon_{xz}\right\}^2\Big]\gamma^2\\ &\quad-\kappa_x^2\kappa_y^2\left(\kappa_y^2-\alpha^2\right)\left(\alpha^2\epsilon_{xx}+2\alpha\beta\epsilon_{xz}\right.\\ &\quad\left.+k_0^2\epsilon_{xz}^2-\kappa_x^2\epsilon_{zz}\right)=0.\end{aligned} \quad (12)$$

The remaining tangential field components are obtained by

$$\begin{cases}\kappa_x^2\tilde{E}_{x1}=-\left(\alpha\beta+k_0^2\epsilon_{xz}\right)\tilde{E}_{z1}-j\omega\mu_0\dfrac{d}{dy}\tilde{H}_{z1}\\ \kappa_y^2\tilde{H}_{x1}=-\alpha\beta\tilde{H}_{z1}+j\omega\epsilon_0\epsilon_{yy}\dfrac{d}{dy}\tilde{E}_{z1}.\end{cases} \quad (13)$$

For $\epsilon_{xz}=0$ and $\epsilon_{xx}=\epsilon_{yy}=\epsilon_{zz}=1$, the wave equations (3) and (4) are reduced to those in the air regions. Their solutions can be easily obtained under the condition that the field components vanish at infinity. Applying the boundary conditions to the tangential field components in each region, we obtain

$$\begin{pmatrix}Y_{xx} & Y_{xz}\\ Y_{zx} & Y_{zz}\end{pmatrix}\begin{pmatrix}\tilde{E}_x(\alpha)\\ \tilde{E}_z(\alpha)\end{pmatrix}=j\omega\mu_0\begin{pmatrix}-\tilde{J}_x(\alpha)\\ \tilde{J}_z(\alpha)\end{pmatrix}. \quad (14)$$

In the above equation, $\tilde{E}_x$ and $\tilde{E}_z$ are the Fourier transforms of the unknown tangential electric field components in the slot: $y=d$, $|x|<w$. $\tilde{J}_x$ and $\tilde{J}_z$ are those of the unknown current components on the conductors: $y=d$, $|x|>w$. The matrix elements are known functions of α and β, and are given in the Appendix.

Galerkin's procedure is applied in order to obtain the determinantal equation for the propagation constant. $\tilde{E}_x$ and $\tilde{E}_z$ are expanded in terms of basis functions as

$$\begin{cases}\tilde{E}_x(\alpha)=\sum\limits_{m=1}^{M}c_m\tilde{\xi}_m(\alpha)\\ \tilde{E}_z(\alpha)=\sum\limits_{n=1}^{N}d_n\tilde{\eta}_n(\alpha)\end{cases} \quad (15)$$

where c_m and d_n are unknown coefficients. The basis functions $\tilde{\xi}_m$ and $\tilde{\eta}_n$ should be the Fourier transforms of appropriately chosen functions, which are, in the present paper,

$$\xi_m(x)=\begin{cases}\cos\{(m-1)\pi x/2w\}/\sqrt{w^2-x^2}, & m=1,3,5,\cdots\\ \sin\{(m-1)\pi x/2w\}/\sqrt{w^2-x^2}, & m=2,4,6,\cdots\end{cases} \quad (16)$$

$$\eta_n(x)=\begin{cases}\sin\{(n+1)\pi x/2w\}/\sqrt{w^2-x^2}, & n=1,3,5,\cdots\\ \cos\{(n-1)\pi x/2w\}/\sqrt{w^2-x^2}, & n=2,4,6,\cdots.\end{cases} \quad (17)$$

Following the usual procedure of the spectral-domain method after substituting (15) into (14), we obtain a system of homogeneous equations:

$$\begin{cases}\sum\limits_{m=1}^{M}K_{pm}^{xx}c_m+\sum\limits_{n=1}^{N}K_{pn}^{xz}d_n=0, & p=1,2,\cdots,M\\ \sum\limits_{m=1}^{M}K_{qm}^{zx}c_m+\sum\limits_{n=1}^{N}K_{qn}^{zz}d_n=0, & q=1,2,\cdots,N\end{cases} \quad (18)$$

for the unknowns c_m and d_n, where

$$\begin{cases}K_{pm}^{xx}=\int_{-\infty}^{+\infty}\tilde{\xi}_p^*(\alpha)Y_{xx}(\beta,\alpha)\tilde{\xi}_m(\alpha)\,d\alpha\\ K_{pn}^{xz}=\int_{-\infty}^{+\infty}\tilde{\xi}_p^*(\alpha)Y_{xz}(\beta,\alpha)\tilde{\eta}_n(\alpha)\,d\alpha\\ K_{qm}^{zx}=\int_{-\infty}^{+\infty}\tilde{\eta}_q^*(\alpha)Y_{zx}(\beta,\alpha)\tilde{\xi}_m(\alpha)\,d\alpha\\ K_{qn}^{zz}=\int_{-\infty}^{+\infty}\tilde{\eta}_q^*(\alpha)Y_{zz}(\beta,\alpha)\tilde{\eta}_n(\alpha)\,d\alpha.\end{cases} \quad (19)$$

TABLE I
CONVERGENCE OF β/k_0 AT 20 GHz FOR SLOTLINE AS A FUNCTION OF THE NUMBER OF BASIS FUNCTIONS FOR A SAPPHIRE SUBSTRATE WITH $\epsilon_{xx}=\epsilon_{zz}=9.4$, $\epsilon_{yy}=11.6$, $\epsilon_{xz}=0$, AND $2w=d=1$ mm

$\eta_n \backslash \xi_m$	1	2	3
1	2.22664	2.22660	2.22660
2	2.22664	2.22660	2.22660
3	2.22665	2.22661	2.22660

TABLE II
CONVERGENCE OF β/k_0 AT 20 GHz FOR MICROSTRIP LINE AS A FUNCTION OF THE NUMBER OF BASIS FUNCTIONS FOR A SAPPHIRE SUBSTRATE WITH $\epsilon_{xx}=\epsilon_{zz}=9.4$, $\epsilon_{yy}=11.6$, $\epsilon_{xz}=0$, AND $2w=d=1$ mm

$\eta_n \backslash \xi_m$	1	2	3
1	3.02017	3.01958	3.01968
2	3.02030	3.01967	3.01966
3	3.02031	3.01968	3.01967

The asterisk in (19) indicates the complex conjugate. The solution which makes the system determinant associated with (18) equal to zero is the desired propagation constant of the eigenmode.

The characteristic impedance of the dominant mode, the other important quantity, is calculated by the following definition:

$$Z_c = V_x^2/2P \tag{20}$$

for the slotline and

$$Z_c = 2P/I_0^2 \tag{21}$$

for the microstrip line, where P is the average power carried in the z direction, V_x the voltage across the slot, and I_0 the total z-directed current on the strip.

III. NUMERICAL RESULTS

In this section, numerical results of the dominant mode in slotlines, as well as in microstrip lines, are presented for a sapphire substrate and a boron nitride one. Computational time critically depends on the number of basis functions used in the numerical calculations. Tables I and II show the convergence of solutions at 20 (GHz) on the number of basis functions for a sapphire substrate with $\epsilon_{xx}=\epsilon_{zz}=9.4$, $\epsilon_{yy}=11.6$, $\epsilon_{xz}=0$, and $2w=d=1$ (mm). The solutions seem to converge with a small number of basis functions both for the slotline and for the microstrip line.

Fig. 2 shows the effective dielectric constants for a sapphire substrate and a boron nitride one without the coordinate misalignment. The structural parameters are chosen as $2w=d=1$ (mm). Fig. 3 shows the corresponding characteristic impedances. The first two even functions for $\tilde{E}_x$ ($\tilde{J}_z$ for microstrip lines) and the first odd function for $\tilde{E}_z$ ($\tilde{J}_x$ for microstrip lines) in (16) and (17) are included in the numerical calculations. For anisotropic crystalline substrates, three different orientations of the principal dielectric axes are possible even in the case without the coordinate misalignment. Therefore, in the figures, three curves are drawn for each substrate material. The dispersion curves for $(\epsilon_{xx},\epsilon_{yy},\epsilon_{zz})=(9.4,11.6,9.4)$ and $(5.12,3.4,5.12)$ in Fig. 2(b) completely overlap with those reported by Kretch and Collin [3, figs. 2 and 6].

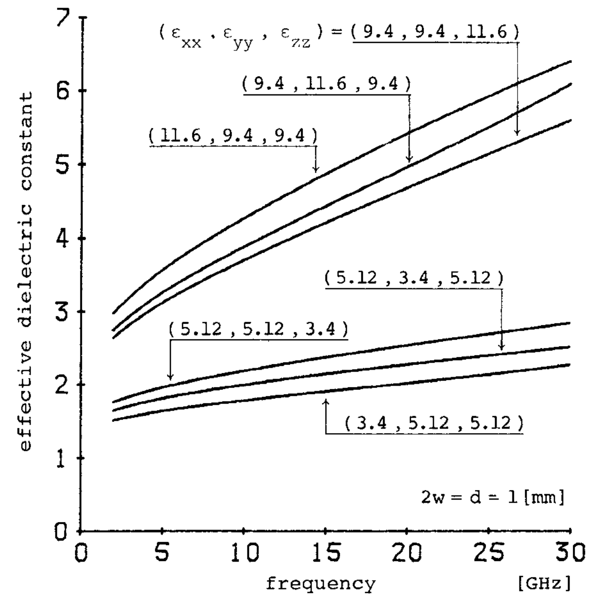

(a)

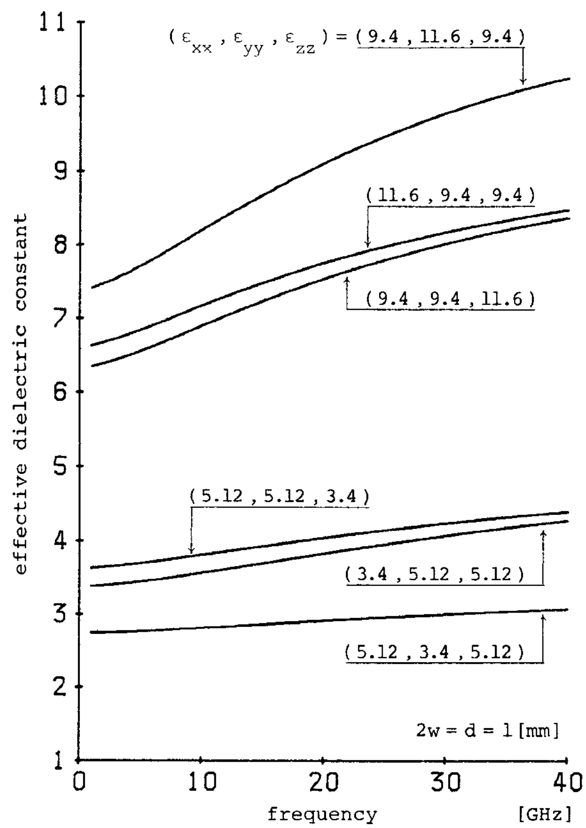

(b)

Fig. 2. Effective dielectric constant for a sapphire substrate and a boron nitride one without coordinate misalignment: (a) slotline and (b) microstrip line.

The dispersion of the effective dielectric constant for a boron nitride substrate with coordinate misalignment and that of the associated characteristic impedance are shown in Fig. 4, where $2w=d=1$ (mm) and $\theta=45°$. The first three functions for $\tilde{E}_x$ ($\tilde{J}_z$ for microstrip lines) and the first odd

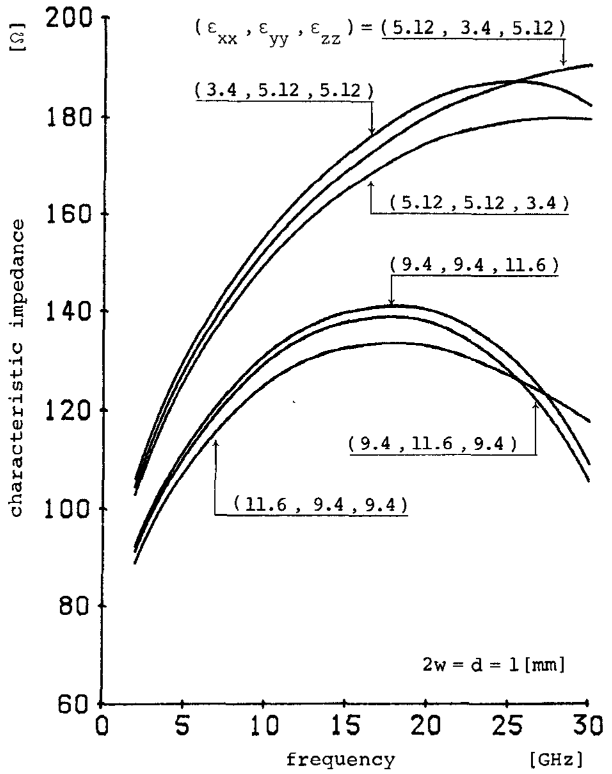

(a)

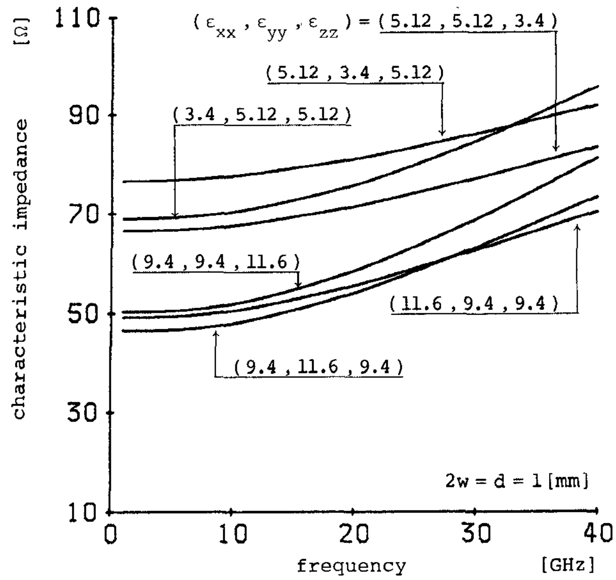

(b)

Fig. 3. Characteristic impedance for a sapphire substrate and a boron nitride one without coordinate misalignment: (a) slotline and (b) microstrip line.

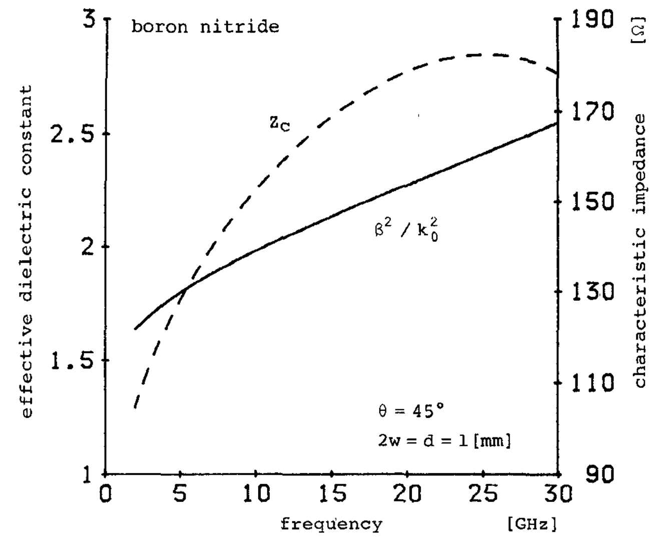

(a)

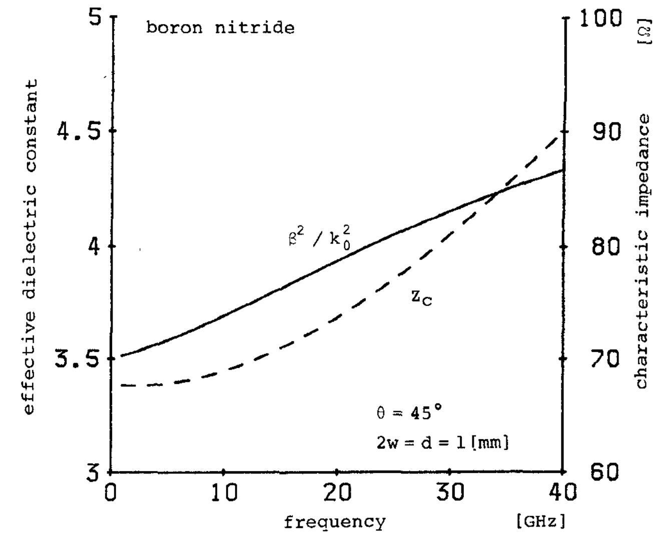

(b)

Fig. 4. Effective dielectric constant and characteristic impedance for a boron nitride substrate with coordinate misalignment: (a) slotline and (b) microstrip line.

function for $\tilde{E}_z$ ($\tilde{J}_x$ for microstrip lines) in (16) and (17) are taken in the numerical calculations in accordance with the convergence check for the basis functions. Each curve falls into the intermediate region bounded by two corresponding curves for $(\epsilon_{xx}, \epsilon_{yy}, \epsilon_{zz}) = (3.4, 5.12, 5.12)$ and $(5.12, 5.12, 3.4)$ in Figs. 2 and 3.

Fig. 5 shows the effective dielectric constant and the characteristic impedance at 20 (GHz) for a boron nitride substrate as a function of oblique angle θ between the optical axis and the z axis. The structural parameters are chosen such that $2w = d = 1$ (mm). With the increase in the oblique angle θ, ϵ_{xx} in (1) decreases according to $\cos 2\theta$. Since E_x is the strongest electric field component of the slotline mode, the effective dielectric constant of it is most strongly influenced by ϵ_{xx} in the dielectric tensor. Therefore, the effective dielectric constant of the mode changes analogously to ϵ_{xx} as the oblique angle is varied. This feature would be found at any operating frequency and structural parameter. On the other hand, for the mode of a microstrip line, E_y is the strongest electric field component. This means that the effective dielectric constant is mainly influenced by ϵ_{yy}, which remains constant to any oblique angle. The E_x component, which senses ϵ_{xx} varying with the oblique angle, is much weaker in its amplitude than the E_y component. This is the reason why the propagation characteristics of

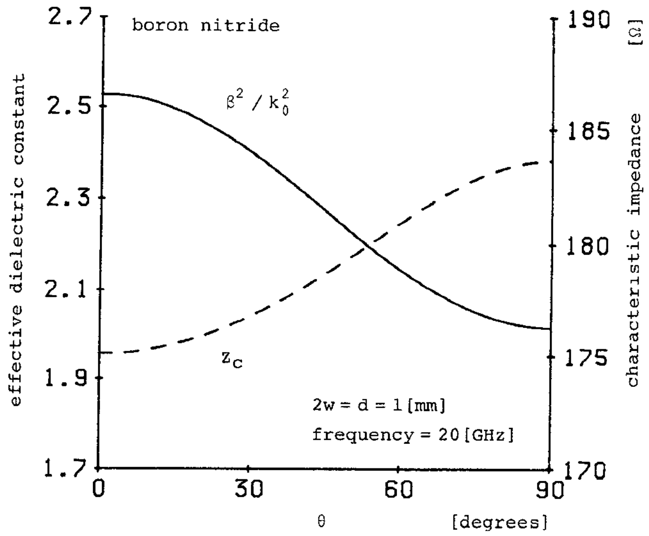

(a)

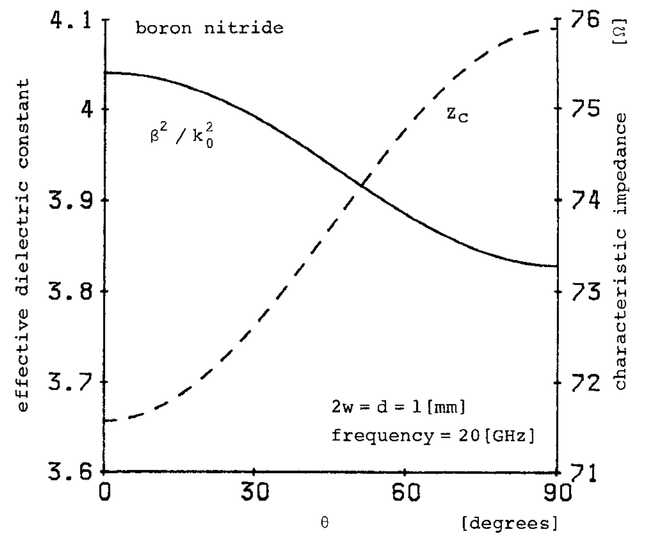

(b)

Fig. 5. Effective dielectric constant and characteristic impedance for a boron nitride substrate as a function of oblique angle: (a) slotline and (b) microstrip line.

slotlines are more sensitive to changes in the oblique angle than those of microstrip lines. The reverse would be true for the coordinate misalignment in the transverse plane.

IV. Conclusions

The propagation characteristics of the dominant mode both in slotlines and in microstrip lines printed on anisotropic substrates are analyzed. The coordinate misalignment on the substrate surface is taken into consideration. The analysis, which is devoted to the slotline, is based on Galerkin's method applied in the spectral domain. Numerical results on the effective dielectric constants and the characteristic impedances are presented for a sapphire substrate and a boron nitride one. It is pointed out that the coordinate misalignment on the substrate surface has a greater influence on the propagation characteristics of the slotline than on those of the microstrip line.

Appendix

$$Y_{xx} = \{\omega\mu_0 Y\kappa_x^2(2S - \omega\epsilon_0 ZN_1) - k_0^2\kappa_x^2(2\omega\epsilon_0 ZR + N_2)\}/\Delta + \kappa_0^2/\gamma_0$$

$$Y_{xz} = \{\omega\mu_0 Y(2SP_1 + Q_1N_1) - k_0^2(P_1N_2 - 2RQ_1)\}/\Delta + \alpha\beta/\gamma_0$$

$$Y_{zx} = \{Q_2\kappa_x^2(-2S + \omega\epsilon_0 ZN_1) + k_0^2P_2\kappa_x^2(2\omega\epsilon_0 ZR + N_2)\}/(\kappa_y^2\Delta) - \alpha\beta/\gamma_0$$

$$Y_{zz} = \{-Q_2(2SP_1 + Q_1N_1) + k_0^2P_2(P_1N_2 - 2RQ_1)\}/(\kappa_y^2\Delta) - \alpha^2\beta^2/(\kappa_0^2\gamma_0) + k_0^2\gamma_0/\kappa_0^2$$

$$\Delta = \{(T_1+T_2)\exp(-\gamma_1-\gamma_2)d + (T_3-T_4)\exp(\gamma_2-\gamma_1)d - (T_3+T_4)\exp(\gamma_1-\gamma_2)d - (T_1-T_2)\exp(\gamma_1+\gamma_2)d\} \cdot k_0^2(\gamma_1 YZ + \gamma_2)$$

$$N_1 = (T_1+T_2)\exp(-\gamma_1-\gamma_2)d + (T_3-T_4)\exp(\gamma_2-\gamma_1)d + (T_3+T_4)\exp(\gamma_1-\gamma_2)d + (T_1-T_2)\exp(\gamma_1+\gamma_2)d$$

$$N_2 = (T_1+T_2)\exp(-\gamma_1-\gamma_2)d - (T_3-T_4)\exp(\gamma_2-\gamma_1)d - (T_3+T_4)\exp(\gamma_1-\gamma_2)d + (T_1-T_2)\exp(\gamma_1+\gamma_2)d$$

$$P_1 = \alpha\beta + \gamma_1\omega\mu_0 Y + k_0^2\epsilon_{xz}$$

$$P_2 = \alpha\beta - \gamma_2\omega\epsilon_0 Z\epsilon_{yy}$$

$$Q_1 = k_0^2\gamma_2 - \omega\epsilon_0 Z(\alpha\beta + k_0^2\epsilon_{xz})$$

$$Q_2 = k_0^2\gamma_1\epsilon_{yy} + \omega\mu_0 Y\alpha\beta$$

$$R = 2\{u(\epsilon_{yy}\gamma_1\kappa_0^2 - \omega\mu_0 Yv/k_0^2) + \omega\mu_0 Y(\omega\mu_0 Yv\gamma_1\kappa_0^2/k_0^2 + \gamma_0^2\kappa_x^2\kappa_y^2 - \epsilon_{yy}\gamma_1^2\kappa_0^4)\}$$

$$S = 2\{\omega\epsilon_0 Zu(v + \omega\epsilon_0 Z\epsilon_{yy}\gamma_2\kappa_0^2) + k_0^2(v\gamma_2\kappa_0^2 - \omega\epsilon_0 Z\gamma_0^2\kappa_x^2\kappa_y^2 + \omega\epsilon_0 Z\epsilon_{yy}\gamma_2^2\kappa_0^4)\}$$

$$T_1 = (1+YZ)\{uv - k_0^2(\gamma_0^2\kappa_x^2\kappa_y^2 + \epsilon_{yy}\gamma_1\gamma_2\kappa_0^4)\} - \kappa_0^2(\gamma_1-\gamma_2)\{\omega\mu_0 Yv + \omega\epsilon_0 Z\epsilon_{yy}u\}$$

$$T_2 = k_0^2\gamma_0\kappa_0^2\{\epsilon_{yy}\kappa_x^2(\gamma_1 + \gamma_2 YZ) + \kappa_y^2(\gamma_2 + \gamma_1 YZ)\}$$

$$T_3 = (1-YZ)\{uv - k_0^2(\gamma_0^2\kappa_x^2\kappa_y^2 - \epsilon_{yy}\gamma_1\gamma_2\kappa_0^4)\} - \kappa_0^2(\gamma_1+\gamma_2)\{\omega\mu_0 Yv - \omega\epsilon_0 Z\epsilon_{yy}u)\}$$

$$T_4 = -k_0^2\gamma_0\kappa_0^2\{\epsilon_{yy}\kappa_x^2(\gamma_1 + \gamma_2 YZ) - \kappa_y^2(\gamma_2 + \gamma_1 YZ)\}$$

$$u = k_0^2\{\alpha\beta(\epsilon_{xx}-1) - \kappa_0^2\epsilon_{xz}\} \qquad v = k_0^2\alpha\beta(\epsilon_{yy}-1)$$

$$\gamma_0^2 = \alpha^2 + \beta^2 - k_0^2 \qquad \kappa_0^2 = k_0^2 - \beta^2.$$

Acknowledgment

The authors wish to thank Mr. Tomochika for his assis tance in the numerical calculations.

References

[1] N. G. Alexopoulos, "Integrated-circuit structures on anisotropic substrates," *IEEE Trans. Microwave Theory Tech.*, vol. MTT-33, pp. 847–881, Oct. 1985.
[2] H-Y. Yang and N. G. Alexopoulos, "Uniaxial and biaxial substrate effects on finline characteristics," *IEEE Trans. Microwave Theory Tech.*, vol. MTT-35, pp. 24–29, Jan. 1987.
[3] B. E. Kretch and R. E. Collin, "Microstrip dispersion including anisotropic substrate," *IEEE Trans. Microwave Theory Tech.*, vol. MTT-35, pp. 710–718, Aug. 1987.
[4] M. R. G. Maia, A. G. D'Assuncao, and A. J. Giarola, "Dynamic analysis of microstrip lines and finlines on uniaxial anisotropic substrates," *IEEE Trans. Microwave Theory Tech.*, vol. MTT-35, pp. 881–886, Oct. 1987.
[5] J. L. Tsalamengas, N. K. Uzunoglu, and N. G. Alexopoulos, "Propagation characteristics of a microstrip line printed on a general anisotropic substrate," *IEEE Trans. Microwave Theory Tech.*, vol. MTT-33, pp. 941–945, Oct. 1985.
[6] T. Itoh and R. Mittra, "Spectral-domain for calculating the dispersion characteristics of microstrip lines," *IEEE Trans. Microwave Theory Tech.*, vol. MTT-21, pp. 496–499, July 1973.

Masahiro Geshiro (S'75–M'78) received the B.E., M.E., and Ph.D. degrees in 1973, 1975, and 1978, respectively, from Osaka University, Osaka, Japan.

In December 1979 he joined the Department of Electronics, Ehime University, Matsuyama, Japan, where he is now an Associate Professor of Electronics Engineering. From March 1986 to January 1987, he was a Visiting Scholar at the University of Texas at Austin, on leave from Ehime University. He has been engaged in research on microwave and optical-wave transmission lines and integrated circuits.

Dr. Geshiro is a member of the Institute of Electronics, Information, and Communication Engineers of Japan.

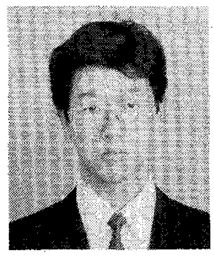

Seikou Yagi was born in Ehime, Japan, on January 22, 1966. He received the B.E. and M.E. degrees in electronics engineering from Ehime University, Ehime, Japan, in 1988 and 1990, respectively.

Since 1990 he has been with NTT Data Communications Systems Corporation, Kanagawa, Japan.

Mr. Yagi is a member of the Institute of Electronics, Information, and Communication Engineers of Japan.

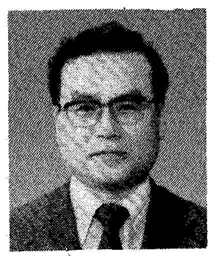

Shinnosuke Sawa (M'72) was born in Osaka, Japan, on October 23, 1938. He received the B.E. degree in electrical engineering from the University of Osaka Prefecture, Osaka, Japan, in 1962 and the M.E. and Ph.D. degrees in electrical communication engineering from Osaka University, Osaka, Japan, in 1967 and 1970, respectively.

From 1962 to 1964 he was with the Mitsubishi Electric Corporation, where he was engaged in ignitron manufacture and vacuum switch development at the corporation's Kyoto plant. Since 1970 he has been with Ehime University, Matsuyama City, Japan. Since 1976 he has been Professor of Electronics Engineering there, and his research has dealt with electromagnetic theory, electromagnetic wave engineering, and optoelectronics. Currently he is doing research on various waveguides from millimeter-wave through optical frequencies and on electromagnetic wave absorbers.

Dr. Sawa is a member of the Institute of Electronics, Information and Communication Engineers of Japan and the Institute of Electrical Engineers of Japan.